



1
2
3
4

FINITE ELEMENT ANALYSIS OF NON-CIRCULAR
HYDRODYNAMIC BEARINGS

M. EL-SHERBINY*, S. ABDELAZIZ**

ABSTRACT

The paper presents the results of a finite element analysis of non circular bearings, such as displaced, half lemon, and spiral bearings.

A number of bearing characteristics are discussed and some geometrical and operational parameters are concluded.

INTRODUCTION

One of the most troublesome features of hydrodynamic journal bearings is the oil whirl [1]. It is a vibration that occurs at a little below half the shaft speed. In curing these problems it is established that a downward hydrodynamic force can increase the natural frequency of the bearing and thereby eliminate or avoid such undesirable feature [1].

There are a number of bearing designs which are known as anti-whip bearings. Falling into this category are the multilobed bearings [2], the half lemon bearings [1], the displaced bearings [3], and the spiral bearings [4].

The only type of these bearing designs which received considerable attention is the multilobed bearings [5]. The present work is therefore devoted to the operational characteristics of the other three types, namely the half lemon, the displaced and the spiral bearings.

The finite element analysis [6] is utilized for solving the incompressible lubrication problem through the variational approach. A limited number of bearings have been investigated in each case, but the program can handle any other bearing with complex geometry.

5

* Associate Prof. Dept. of Mech. Design, Cairo University, Cairo, Egypt.

** Lt. Colonel, Egyptian Army.

FINITE ELEMENT FORMULATION.

In utilizing the variational approach [7] in solving the Reynolds equation,

$$\frac{\partial}{\partial x} \left(\frac{h^3}{6\eta} \frac{\partial p}{\partial x} \right) + \frac{\partial}{\partial y} \left(\frac{h^3}{6\eta} \frac{\partial p}{\partial y} \right) = U \frac{dh}{dx} \quad (1)$$

The problem reduces to minimizing an equivalent function

$$J(p(x,y)) = \int_A \left[\frac{-h^3}{12\eta} \left(\frac{\partial p}{\partial x} \right)^2 - \frac{h^3}{12\eta} \left(\frac{\partial p}{\partial y} \right)^2 + hU_x \frac{\partial p}{\partial x} \right] dA \quad (2)$$

within a well defined solution domain subject to a nonvanishing boundary condition:

$$p = P(x,y) \quad (3)$$

on a nonvanishing boundary segment S_p and a flow boundary condition:

$$Q = \hat{n} \left[\frac{u_x h}{2} - \frac{h^3}{12\eta} \left(\frac{\partial p}{\partial x} + \frac{\partial p}{\partial y} \right) \right] \quad (4)$$

on a boundary segment S_q

MODELING

The bearing surface is divided into N , ($N = N_C \times N_L$) rectangular elements. If elements of equal dimensions are considered then

$$\Delta x = 2\pi R / N_C \quad \text{and} \quad \Delta y = L / N_L$$

Finer elements however are generally used in areas of steep pressure gradients. The total number of the rectangular elements was limited to 200 to match the capacity of the employed computer. The program however was designed to include further refinement by dividing each rectangular element into four triangular elements of three nodes each.

The film thickness distribution was initially calculated from the bearing geometry at preselected eccentricities.

The program was usually checked for accuracy [8] by solving a problem for which a solution is known.

RESULTS

Half Lemon Bearings

In the present work, bearings having clearance ratio (C_s) between 2.5 and 3 with concentric lower shells and aspect ratios (L/D) of 0.5, 1.0 and 1.5 are considered. Fig.1 shows the geometry of the bearing, while Fig.2 shows the pressure distribution obtained for a square bearing ($L/D = 1.0$) at an

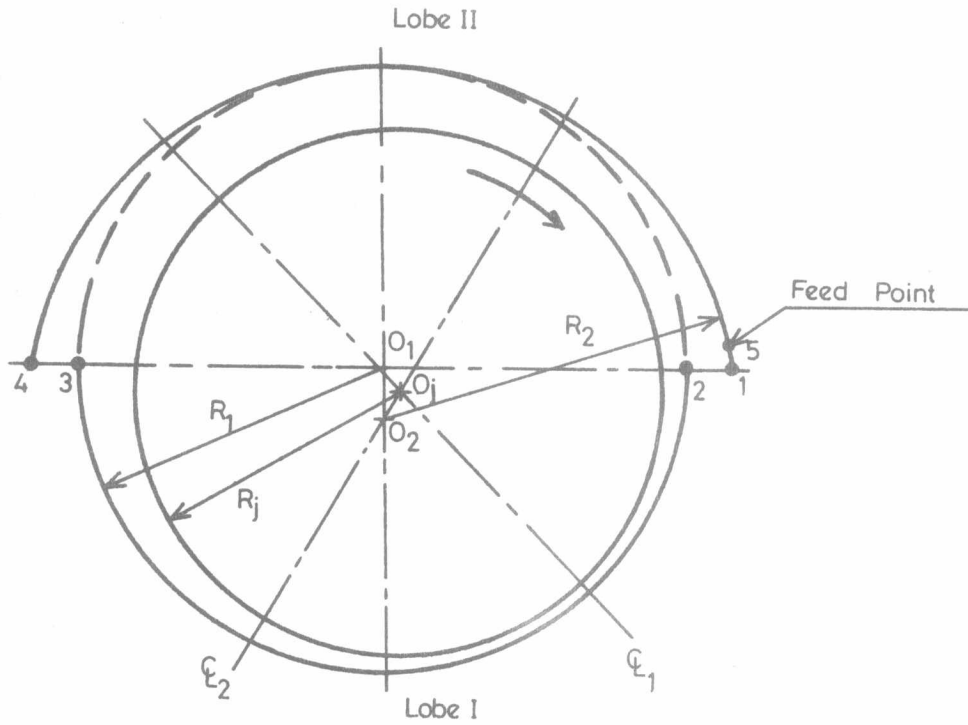


Fig:1 GEOMETRY OF HALF-LEMON BEARING

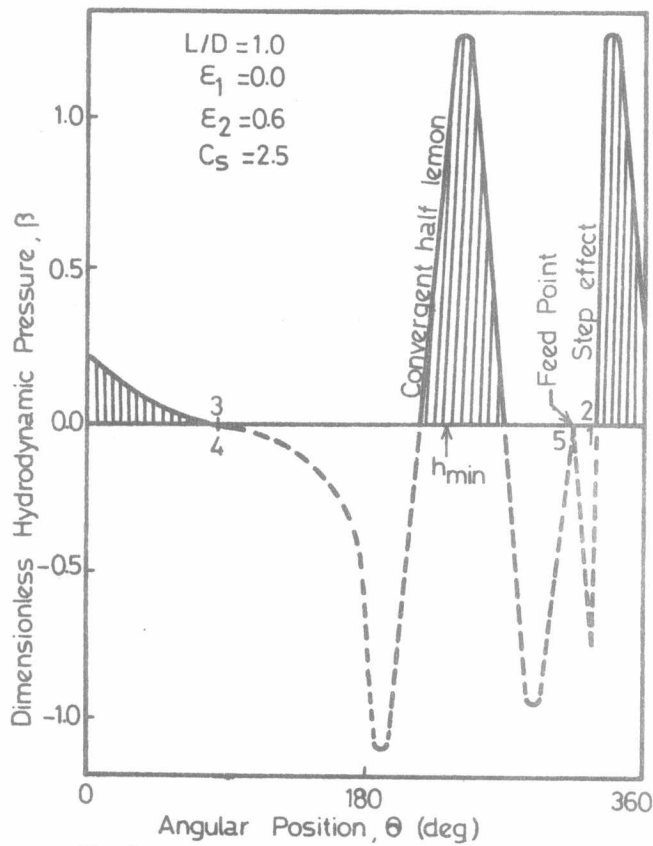


Fig:2 PRESSURE DISTRIBUTION OF HALF-LEMON BEARING

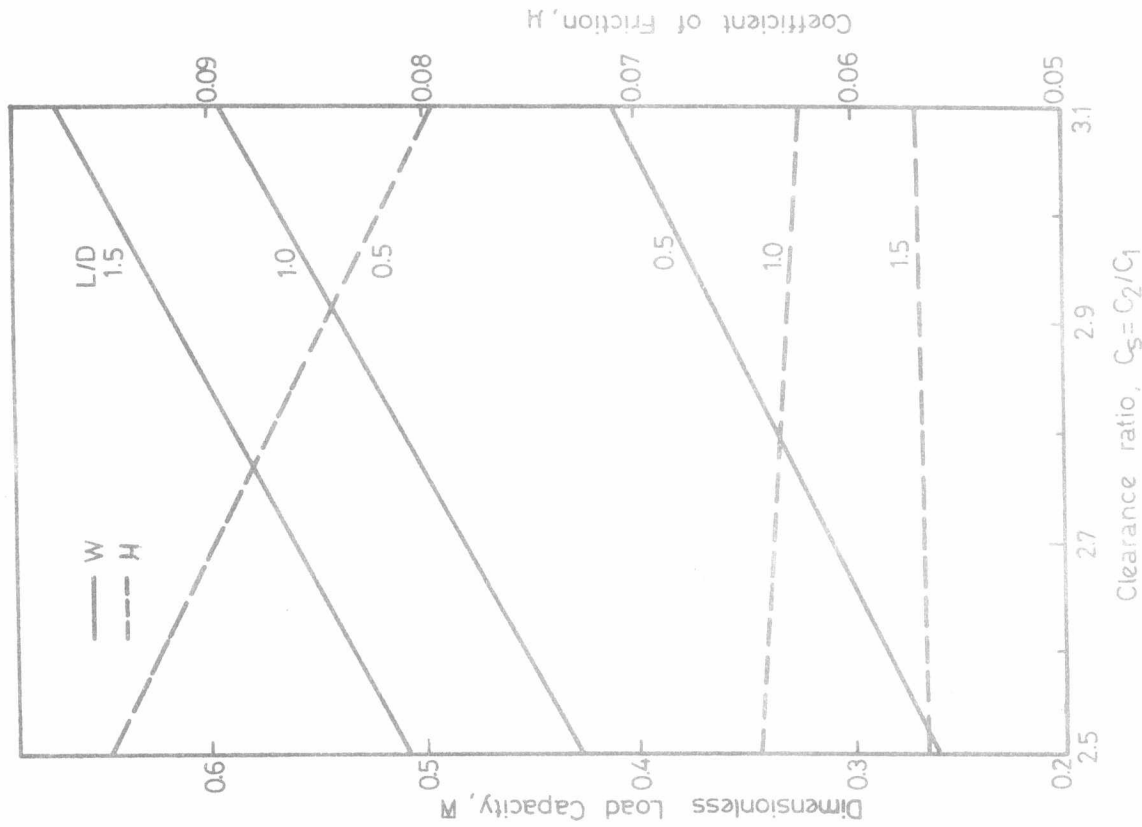


Fig:3 LOAD CAPACITY AND COEFFICIENT OF FRICTION VS CLEARANCE RATIO.

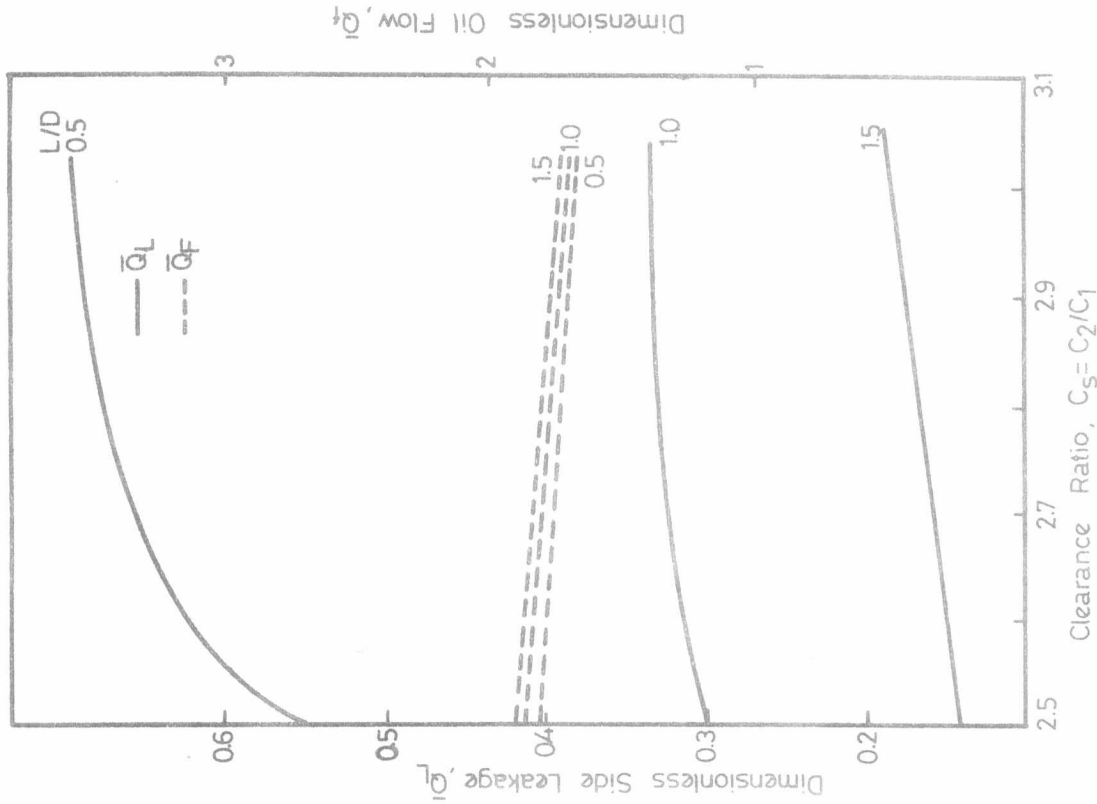


Fig:4 OIL FLOW AND SIDE LEAKAGE VS CLEARANCE RATIO.

upper eccentricity ratio of 2.5. The dimensionless load capacity (\bar{W}) and coefficient of friction (μ) obtained at different clearance ratios are also shown in Fig.3, while the corresponding dimensionless oil flow (\bar{Q}_f) and side leakage \bar{Q}_L are shown in Fig.4. Because of the too many design variables involved, a large number of computer runs are required to fully characterize such bearings. The present results however are only a representative sample of the available data.

Displaced Bearings

Bearings having relative lateral displacements ($R_d = D_s/R$) within the range 0.004 up to 0.006 but with different aspect ratios (L/D) of 0.5, 1.0, and 1.5 has just been investigated. Full characterization of displaced bearings still requires a tremendous amount of computer work; and we can only give a representative sample of the results.

Fig.5 shows the basic geometrical features of the displaced bearings, while Fig.6 shows the pressure distribution in two runs with different eccentricities ratio ($\epsilon_r = \epsilon_2/\epsilon_1$). In Fig.7 the dimensionless load capacity and coefficient of friction $\bar{\mu}$ are presented for bearings of equal eccentricities ($\epsilon_2 = \epsilon_1$), and in Fig.8 the same results obtained for square bearings having different relative eccentricities are illustrated. The oil flow rates are also shown in Fig.9. A critical relative eccentricity ratio (ϵ_r) is found for each relative displacement (R_d) below which the load carrying capacity would generally decrease, see for example Fig.10. This figure can be used as a design guide for minimizing or eliminating oil whirl.

Spiral Bearings.

Spiral bearings having clearances ratio within the range 2-30 are considered. Fig.11 shows the bearing geometry, while Fig.12 shows the pressure distribution at a relative clearance of 2.5. The computed load capacity \bar{W} and friction (μ) are also shown in Fig.13 for different clearance ratios. Fig. 14 shows a carpet plot for the computed friction interms of relative clearance (C_s) and the eccentricity ratios of the two halves. Fig.15 shows similar results for the computed load capacity (\bar{W}), while Fig.16 shows the corresponding side leakage values.

CONCLUSION

The finite element analysis is shown to be able to handle bearings of complex geometry, such as half lemon, displaced and spiral bearings.

Some operational data of each of the above mentioned bearings is reported, and a critical eccentricity ratio chart is produced to assist designers in minimizing bearing whirl.

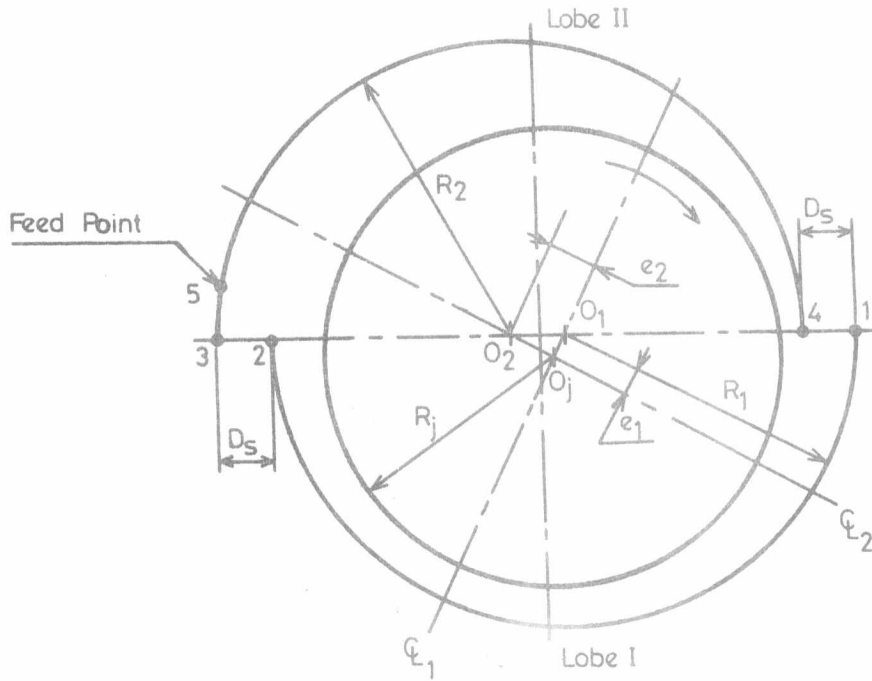


Fig:5 GEOMETRY OF DISPLACED BEARING

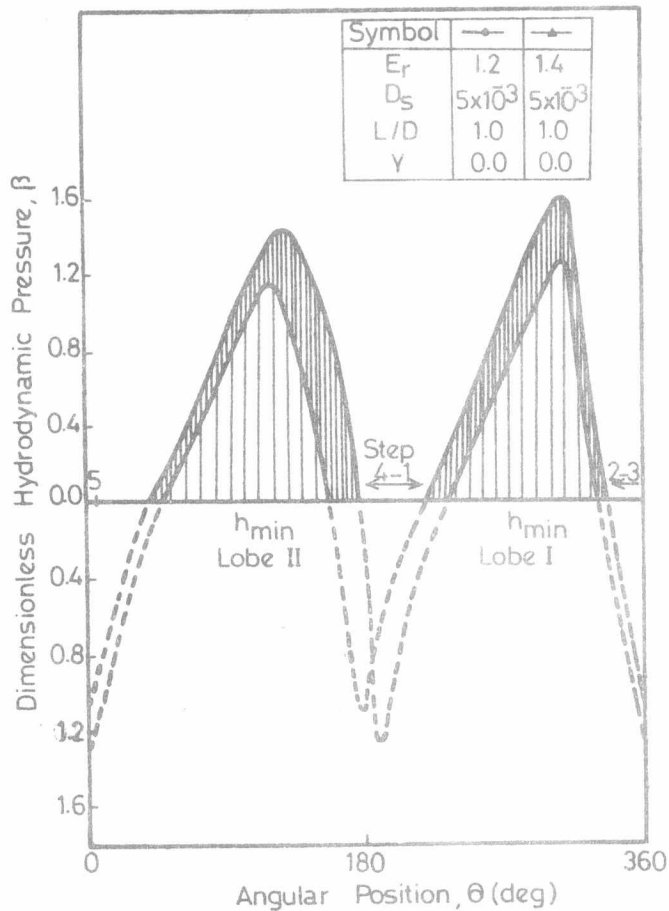


Fig:6 PRESSURE DISTRIBUTION OF DISPLACED BEARINGS

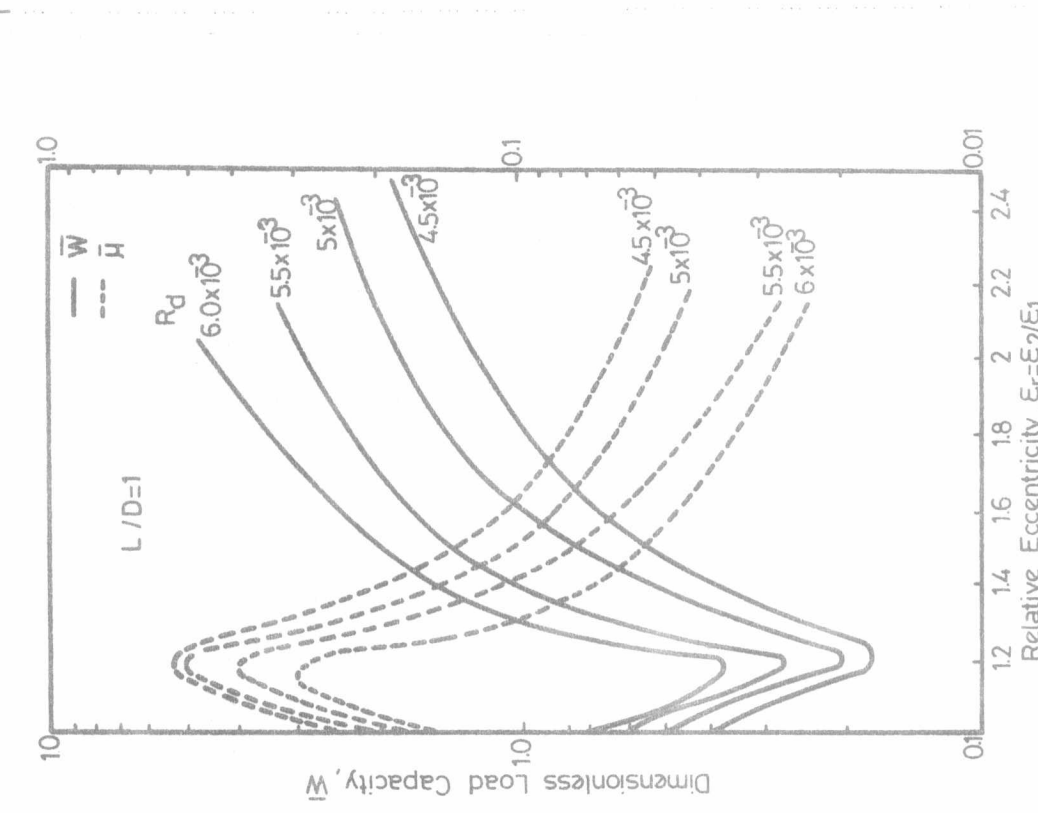


Fig.8 LOAD CAPACITY AND COEFFICIENT OF FRICTION VS RELATIVE ECCENTRICITY.

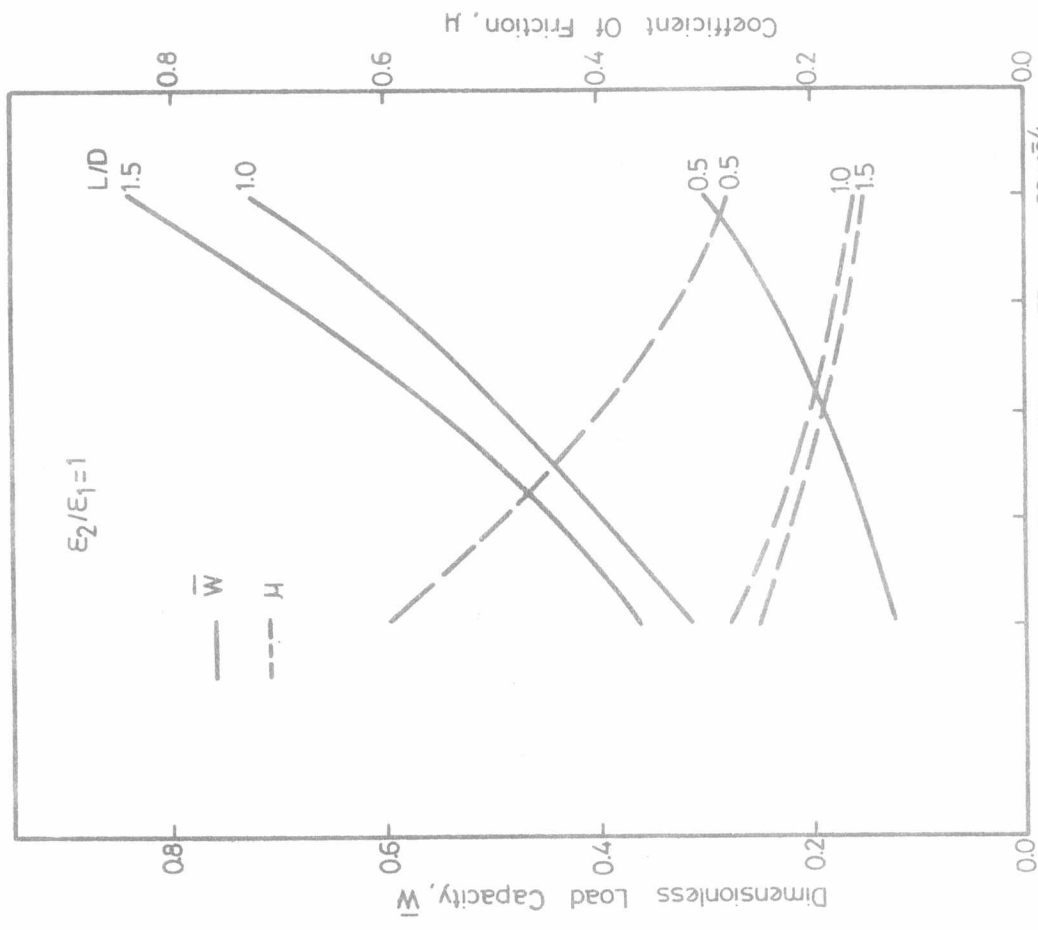


Fig:7 LOAD CAPACITY AND COEFFICIENT OF FRICTION VS RELATIVE DISPLACEMENT

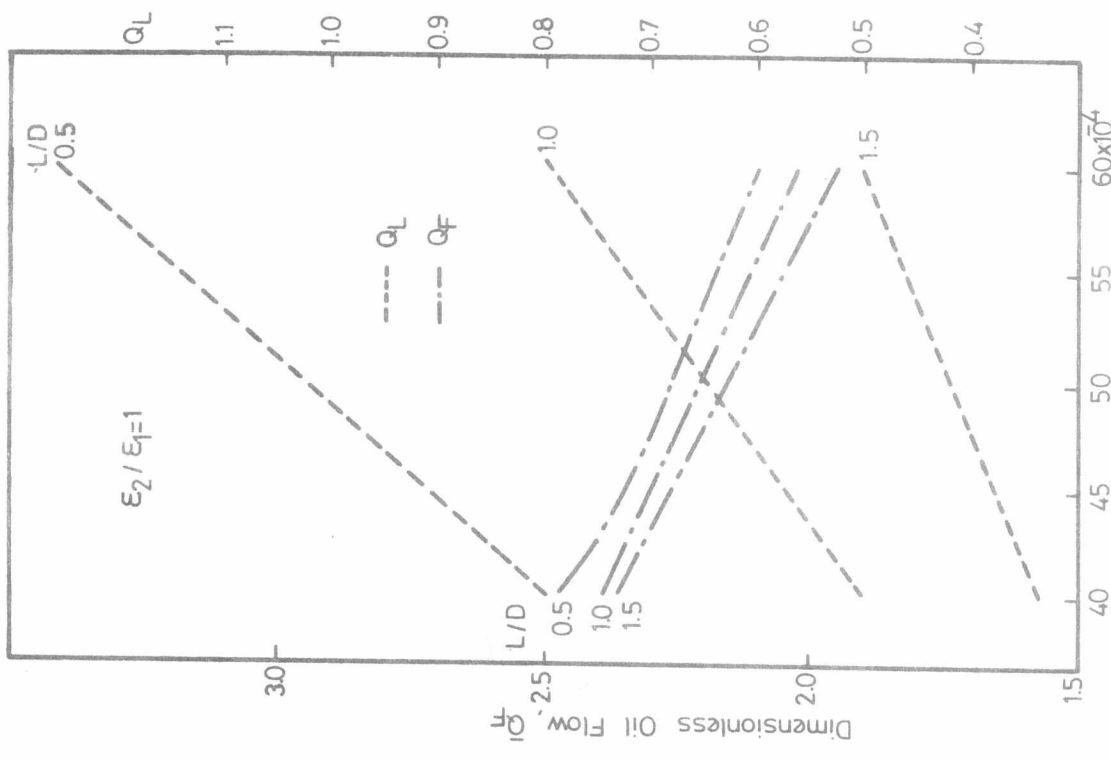


Fig.9 MODIFIED SOMMERFELD NUMBER, OIL FLOW AND SIDE LEAKAGE VS RELATIVE DISPLACEMENT

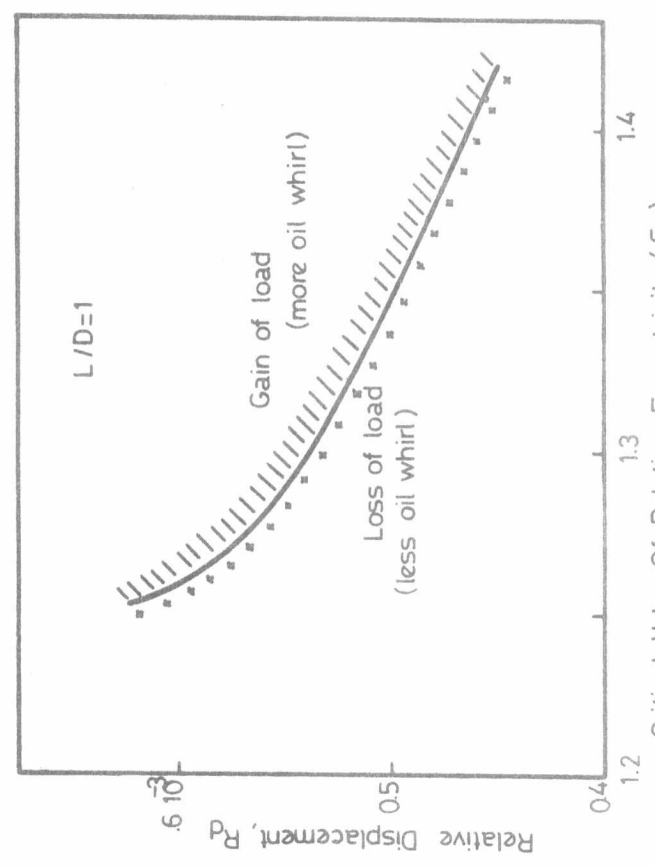


Fig.10 RELATIVE DISPLACEMENT VS CRITICAL VALUE OF RELATIVE ECCENTRICITY

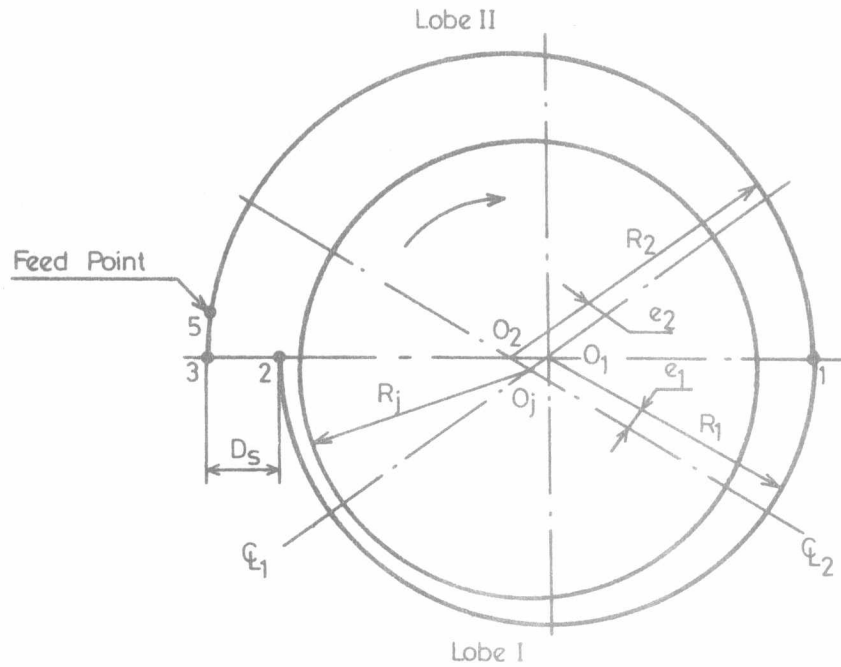


Fig:11 GEOMETRY OF SPIRAL BEARING

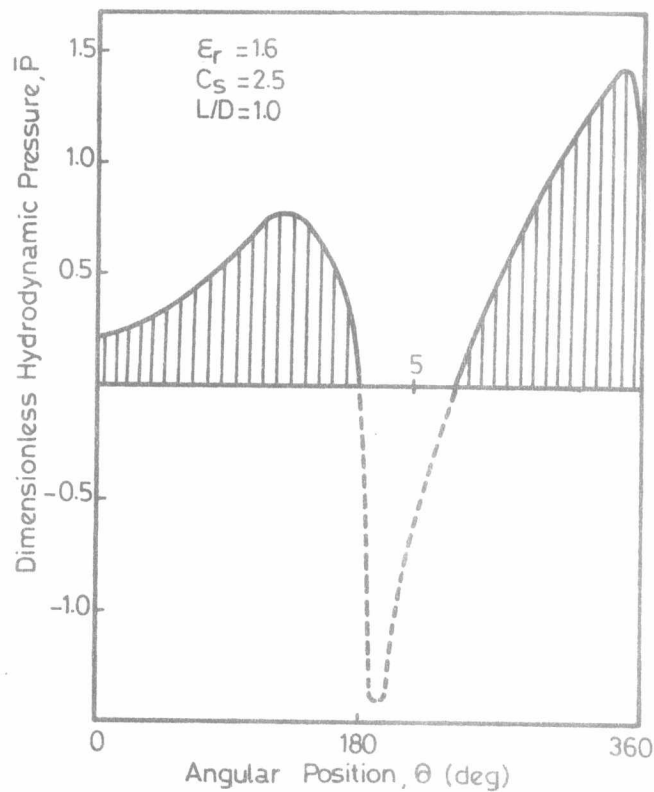


Fig:12 PRESSURE DISTRIBUTION OF SPIRAL BEARING

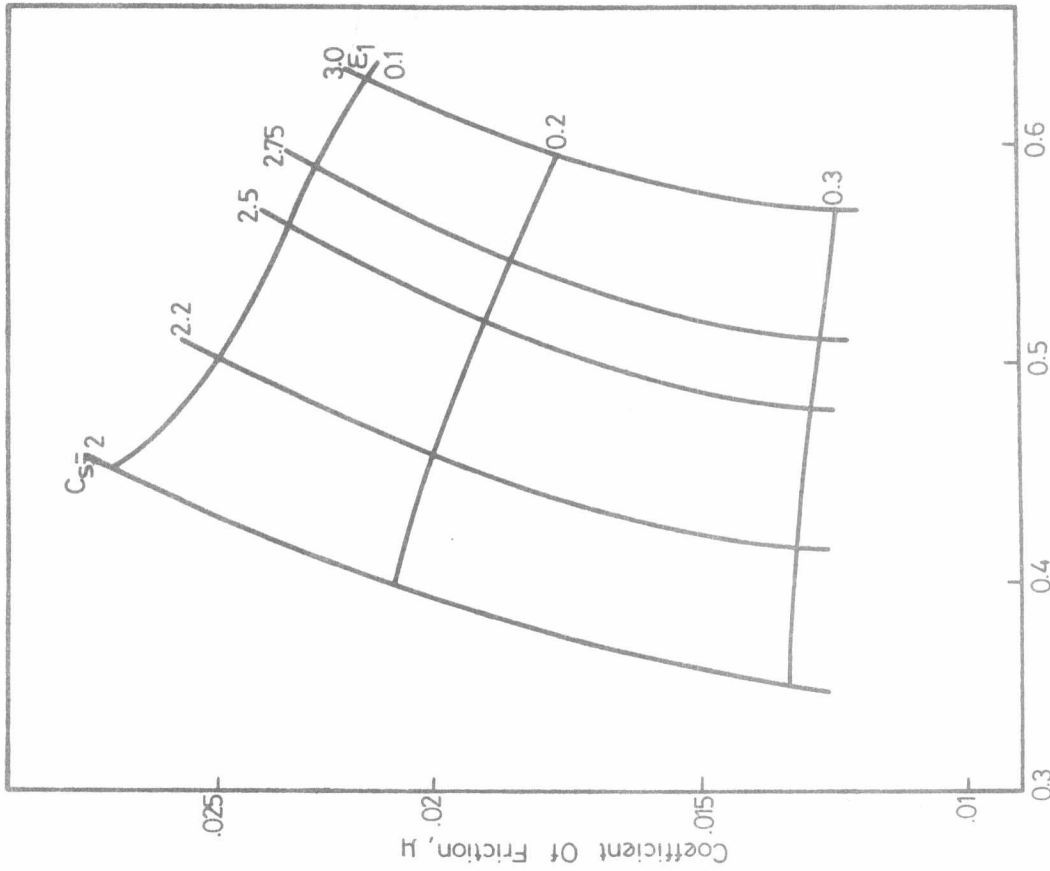


Fig:14 COEFFICIENT OF FRICTION AND ECCENTRICITY RATIOS RELATIONSHIP

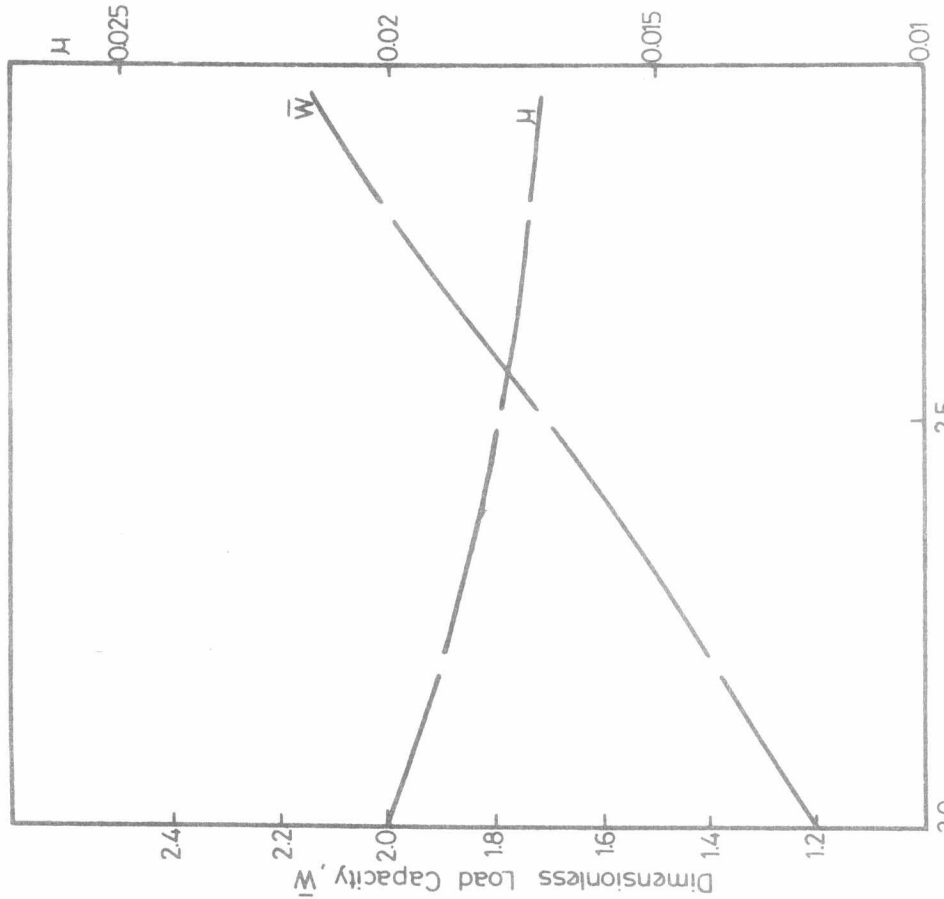


Fig:13 LOAD CAPACITY, MODIFIED SOMMERFELD NUMBER AND COEFFICIENT OF FRICTION VS RELATIVE CLEARANCE.

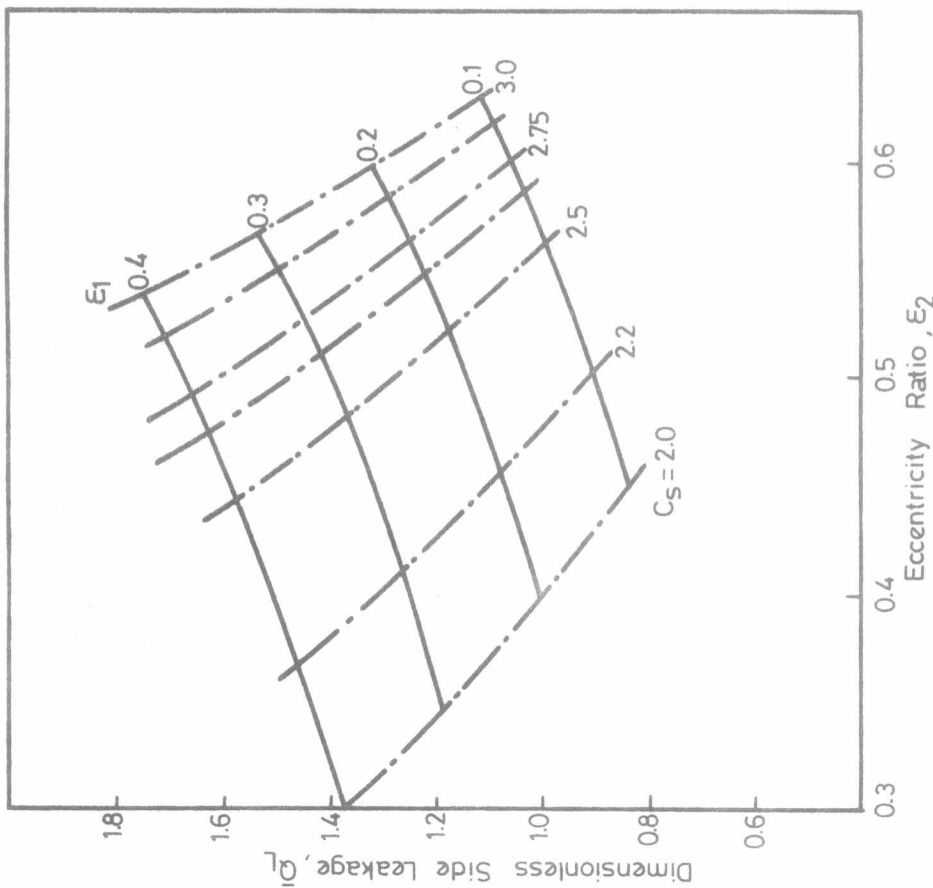


Fig:16 SIDE LEAKAGE AND ECCENTRICITY RATIOS RELATIONSHIP

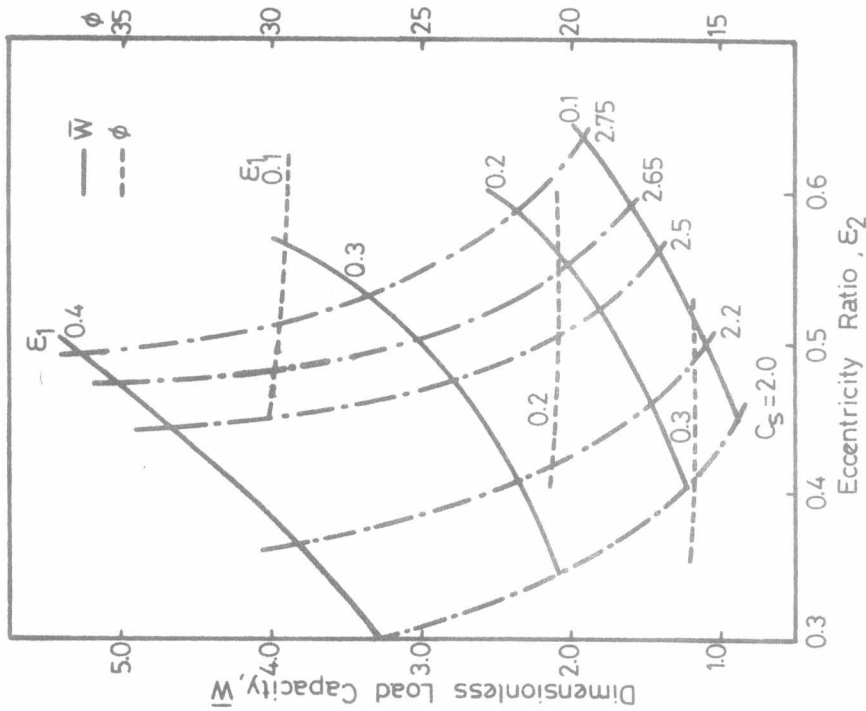


Fig:15 LOAD CAPACITY AND ATTITUDE ANGLE AT DIFFERENT ECCENTRICITY RATIOS (1 AND 2)

Considerable amount of computational work is still required before these bearings can be fully characterized.

REFERENCES

- [1] Cameron, A. "Basic Lubrication Theory", Longman, London, 129-133, (1970).
- [2] Li, D, Choy, K. and Allaire, P. "Stability and Transient Characteristics of Four Multilobe Journal Bearings," Trans. ASME, J. Lub. Tech., 102, 291-299, (1980).
- [3] Wilcock, D, "Analysis of Displaced Bearing," Trans. ASLE, 4, 117-118, (1961).
- [4] Glacier Metal Co, "Spiral Bearings," A British Patent Dec. 17, 1952, No. 247-684, (1952).
- [5] Li, D., Choy, K. and Allaire, P. "Transient Unbalance Response of Four Multilobe Journal Bearings," Trans. ASME, J. Lub. Tech., 102, 300-307, (1980).
- [6] Abdelaziz, S, "Finite Element Analysis of Hydrodynamic Bearings," M.Sc. Thesis, Dept. of Mech. Design, Cairo University, Cairo, Egypt, (1981).
- [7] Hays, D, "A Variational Approach to Lubrication Problems," Trans. ASME, J. Basic Engg., 13-23, (1959).
- [8] El-Sherbiny, M, and Abdelaziz "Finite Element Analysis of Hydrodynamic Bearings," Accepted for Publication in AMSE periodical, (1984).

NOMENCLATURE

C	Radial clearance between journal and shell
C_s	Clearance ratio (C_2/C_1)
D_s	Lateral displacement of displaced bearing
e	eccentricity
h	Film thickness
L	Bearing length
N_c	Number of elements in circumferential direction
N_L	Number of elements in axial
P	Pressure
\bar{Q}_f	Dimensionless oil flow = $[Q/(R_j C N_L)]$
\bar{Q}_L	Dimensionless side leakage = $[Q_L/(R_j C N_L)]$
R	Radius of shell
R_j	Radius of journal
S	Sommerfeld number ($\eta N_L D R^2 / W C^2$)
U	Bearing velocity
W	Dimensionless load = $[W(C/R)^2 / \eta R N]$

